COMPARATIVE VISION

Vision using multiple distinct rod opsins in deep-sea fishes

Zuzana Musilova[1,2]*†, Fabio Cortesi[1,3]*†, Michael Matschiner[1,4,5], Wayne I. L. Davies[6,7,8,9]‡, Jagdish Suresh Patel[10,11], Sara M. Stieb[1,3,12], Fanny de Busserolles[3,13], Martin Malmstrøm[1,4]§, Ole K. Tørresen[4], Celeste J. Brown[11], Jessica K. Mountford[6,7,8], Reinhold Hanel[14], Deborah L. Stenkamp[11], Kjetill S. Jakobsen[4], Karen L. Carleton[15], Sissel Jentoft[4], Justin Marshall[3], Walter Salzburger[1,4]†

Vertebrate vision is accomplished through light-sensitive photopigments consisting of an opsin protein bound to a chromophore. In dim light, vertebrates generally rely on a single rod opsin [rhodopsin 1 (RH1)] for obtaining visual information. By inspecting 101 fish genomes, we found that three deep-sea teleost lineages have independently expanded their *RH1* gene repertoires. Among these, the silver spinyfin (*Diretmus argenteus*) stands out as having the highest number of visual opsins in vertebrates (two cone opsins and 38 rod opsins). Spinyfins express up to 14 *RH1*s (including the most blueshifted rod photopigments known), which cover the range of the residual daylight as well as the bioluminescence spectrum present in the deep sea. Our findings present molecular and functional evidence for the recurrent evolution of multiple rod opsin–based vision in vertebrates.

Animals use vision for a variety of fundamental tasks, including navigation, foraging, predator avoidance, and mate choice. At the molecular level, the process of vision is initiated through a light-induced conformational change in a photopigment (a visual opsin bound to a vitamin A–derived chromophore), which in turn activates the phototransduction cascade (*1*). Vertebrates possess up to five types of visual opsins, four of which are primarily expressed in cone photoreceptors in the retina and one in the rod photoreceptor (*1*). Cones generally operate in bright-light (photopic) conditions and are sensitive to a broad range of wavelengths: Photopigments containing the short-wavelength–sensitive opsins, SWS1 and SWS2, absorb in the ultraviolet [peak spectral sensitivity (λ_{max}) = 355 to 450 nm] and violet-blue (λ_{max} = 415 to 490 nm) regions of the spectrum, respectively; the middle-wavelength–sensitive opsin rhodopsin 2 (RH2) is most sensitive to the central (green) waveband (λ_{max} = 470 to 535 nm); and the long-wavelength–sensitive opsin LWS is tuned to the spectrum's red end (λ_{max} = 490 to 570 nm) (*1*). Usually, vertebrates rely on two to four spectrally distinct cone photoreceptors for color opponency (the ability to distinguish different chromatic signals) (*2*, *3*). Under dim-light (scotopic) conditions, most vertebrates are color-blind and rely on their single rod photopigment (RH1) for obtaining achromatic visual information (*1*, *3*).

In this study, we scrutinized the evolution of the visual opsin gene repertoire of teleosts, with a particular focus on deep-sea fishes. These animals exhibit various adaptations to maximize their visual sensitivities in a scotopic environment where bioluminescence replaces surface illumination as the primary source of light (*4*, *5*); their adaptations include increased eye or pupil sizes, reflective tapeta, and extremely modified tubular eye structures (*6*). Other modifications concern the retina itself, with many deep-sea fishes having pure-rod retinae with elongated outer segments and, in some cases, multibank retinae in which rods are stacked in layers (*7*).

To examine molecular adaptations in the teleost visual system, we first reconstructed the visual opsin gene loci in 100 teleosts, as well as one nonteleost outgroup (Fig. 1, fig. S1, and table S1) (*8*). We found that teleosts possess a median number of seven visual opsin genes. This number is elevated compared with that of other vertebrates (*3*) and can primarily be attributed to expansion of *SWS2* and *RH2*, which are sensitive to the most prevalent, blue-green part of the aquatic light spectrum. We found that 78 species had more than one *RH2* copy, and 53 species had at least one extra version of *SWS2* [see also (*9*)]. Gene losses, on the other hand, mainly affected opsins *SWS1* (absent in 46 species) and *LWS* (absent in 34 species, of which 28 inhabit the deep sea), which are sensitive to the edges of the visible light spectrum.

A phylogenetic generalized least-squares (PGLS) analysis revealed that although the total number of visual opsin genes was unaffected by phylogeny or the depth at which a species occurs (Pagel's λ = 0, $F_{1,74}$ = 0.32, P = 0.57), deeper-dwelling species have significantly fewer *LWS* genes (Pagel's λ = 1.0, $F_{1,74}$ = 38.47, P < 0.0001) (table S2). In common with most vertebrates (*3*), the majority of teleosts possess a single *RH1*, irrespective of phylogeny and depth (Pagel's λ = 0, $F_{1,74}$ = 2.87, P = 0.09). However, we identified 13 species with more than one *RH1* [see also (*10*)]. Notably, four deep-sea species from three distinct clades possess five or more *RH1*s: the glacier lanternfish (*Benthosema glaciale*) with 5 *RH1*s; the tube-eye (*Stylephorus chordatus*) with 6 *RH1*s; and two species of the Diretmidae, the longwing spinyfin (*Diretmoides pauciradiatus*) with 18 *RH1*s and the silver spinyfin (*Diretmus argenteus*) with 38 *RH1*s (Fig. 1). In all cases, the *RH1* gene expansions occurred through single-gene rather than whole-genome duplications (fig. S2 and table S3).

To determine which of the visual opsins are being used, we sequenced retinal transcriptomes of 36 species sampled across the teleost phylogeny. We found that the majority of species (n = 24) express up to four cone opsins, despite in many cases having more opsin genes in their genomes (fig. S3). This finding is consistent with the fact that most vertebrates use two to four differently tuned cone photoreceptors for color vision (*11*). The retinae of the remaining 12 species contained transcripts of five to seven cone opsins (fig. S3), a pattern previously reported in some teleosts (*3*). We further found that deep-sea fishes with an extended *RH1* repertoire express more than one *RH1*: The lanternfishes *B. glaciale* and *Ceratoscopelus warmingii* express three *RH1*s each, the tube-eye expresses five *RH1*s, and silver spinyfins express up to 7 and 14 *RH1*s as larvae and adults, respectively (Fig. 2A and table S4). A similarly high number of retinal opsin transcripts has previously been reported only for dragonflies (*12*) and stomatopod crustaceans (*13*), the latter of which can generate up to 12 differently tuned photoreceptor types.

In vertebrates, substitutions at 27 amino acid positions have so far been implicated with the

[1]Zoological Institute, Department of Environmental Sciences, University of Basel, Basel, Switzerland. [2]Department of Zoology, Faculty of Science, Charles University, Prague, Czech Republic. [3]Queensland Brain Institute, The University of Queensland, Brisbane, QLD, Australia. [4]Centre for Ecological and Evolutionary Synthesis (CEES), Department of Biosciences, University of Oslo, Oslo, Norway. [5]Department of Palaeontology and Museum, University of Zurich, Zurich, Switzerland. [6]UWA Oceans Institute, The University of Western Australia, Perth, WA, Australia. [7]School of Biological Sciences, The University of Western Australia, Perth, WA, Australia. [8]Lions Eye Institute, The University of Western Australia, Perth, WA, Australia. [9]Oceans Graduate School, The University of Western Australia, Perth, WA, Australia. [10]Center for Modeling Complex Interactions, University of Idaho, Moscow, ID, USA. [11]Department of Biological Sciences, University of Idaho, Moscow, ID, USA. [12]Center for Ecology, Evolution and Biogeochemistry, Department of Fish Ecology and Evolution, Swiss Federal Institute of Aquatic Science and Technology (EAWAG), Kastanienbaum, Switzerland. [13]Red Sea Research Center (RSRC), Biological and Environmental Sciences and Engineering Division (BESE), King Abdullah University of Science and Technology (KAUST), Thuwal, Saudi Arabia. [14]Thünen Institute of Fisheries Ecology, Bremerhaven, Germany. [15]Department of Biology, University of Maryland, College Park, MD, USA.
*These authors contributed equally to this work.
†Corresponding authors. Email: zuzana.musilova@natur.cuni.cz (Z.M.); fabio.cortesi@uqconnect.edu.au (F.C.); walter.salzburger@unibas.ch (W.S.) ‡Present address: Umeå Centre for Molecular Medicine (UCMM), Umeå University, Umeå, Sweden. §Present address: Norwegian Scientific Committee for Food and Environment, Oslo, Norway.

Downloaded from http://science.sciencemag.org/ on May 9, 2019

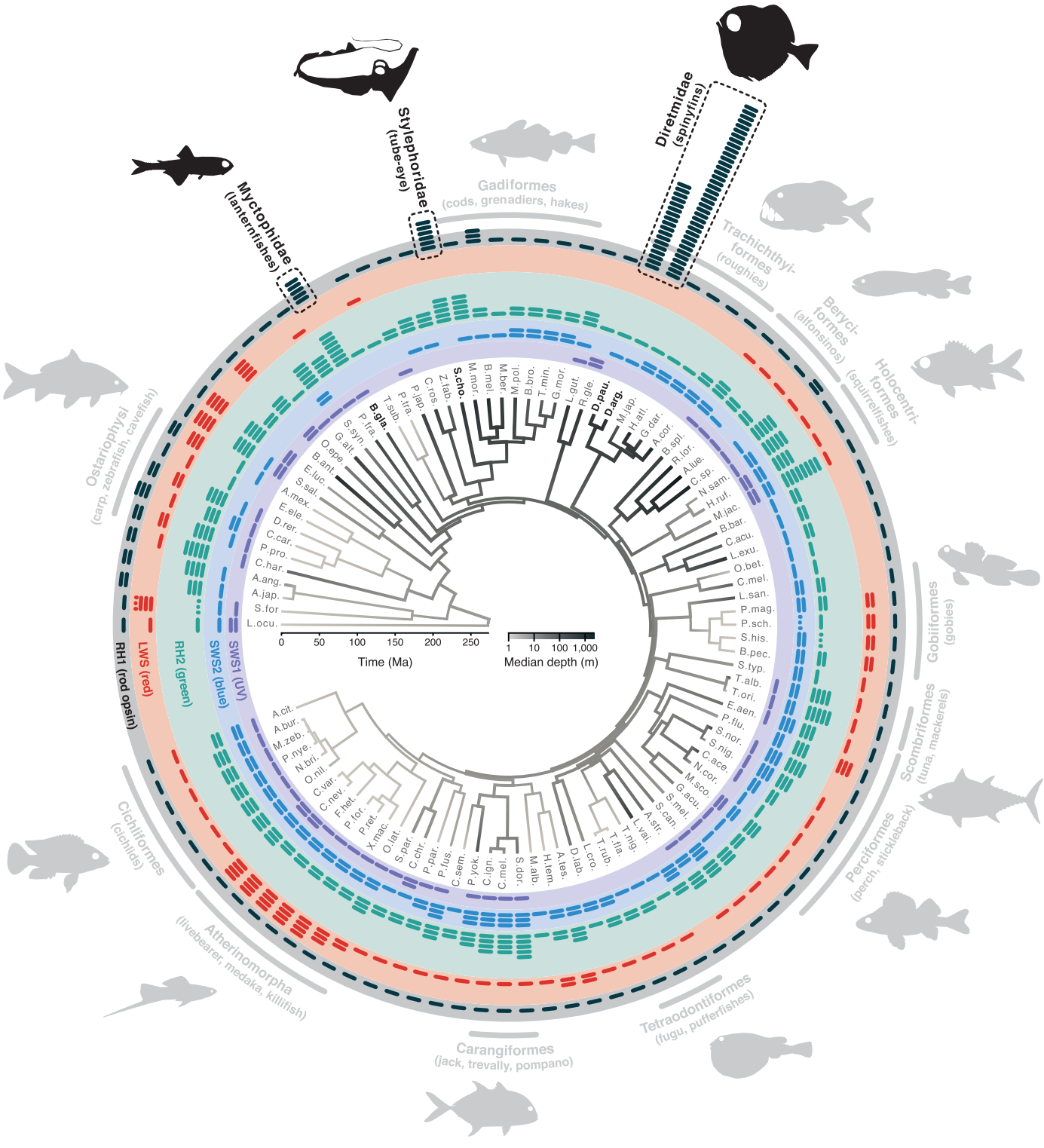

Fig. 1. Diversity of visual opsin genes in teleost fishes. The time-calibrated phylogeny in the center is based on molecular information from 101 fish genomes and is shaded according to the median depth of occurrence of each species (terminal branches) and reconstructed depths (internal branches). Colored bars in the outer circles indicate the number of cone opsin genes, black bars represent the number of rod opsins (*RH1*s), and dotted bars denote incomplete or ambiguous data. Deep-sea lineages with multiple *RH1* copies are highlighted with dashed boxes. A detailed version of the phylogeny, including full species names, is provided in fig. S1.

Downloaded from http://science.sciencemag.org/ on May 9, 2019

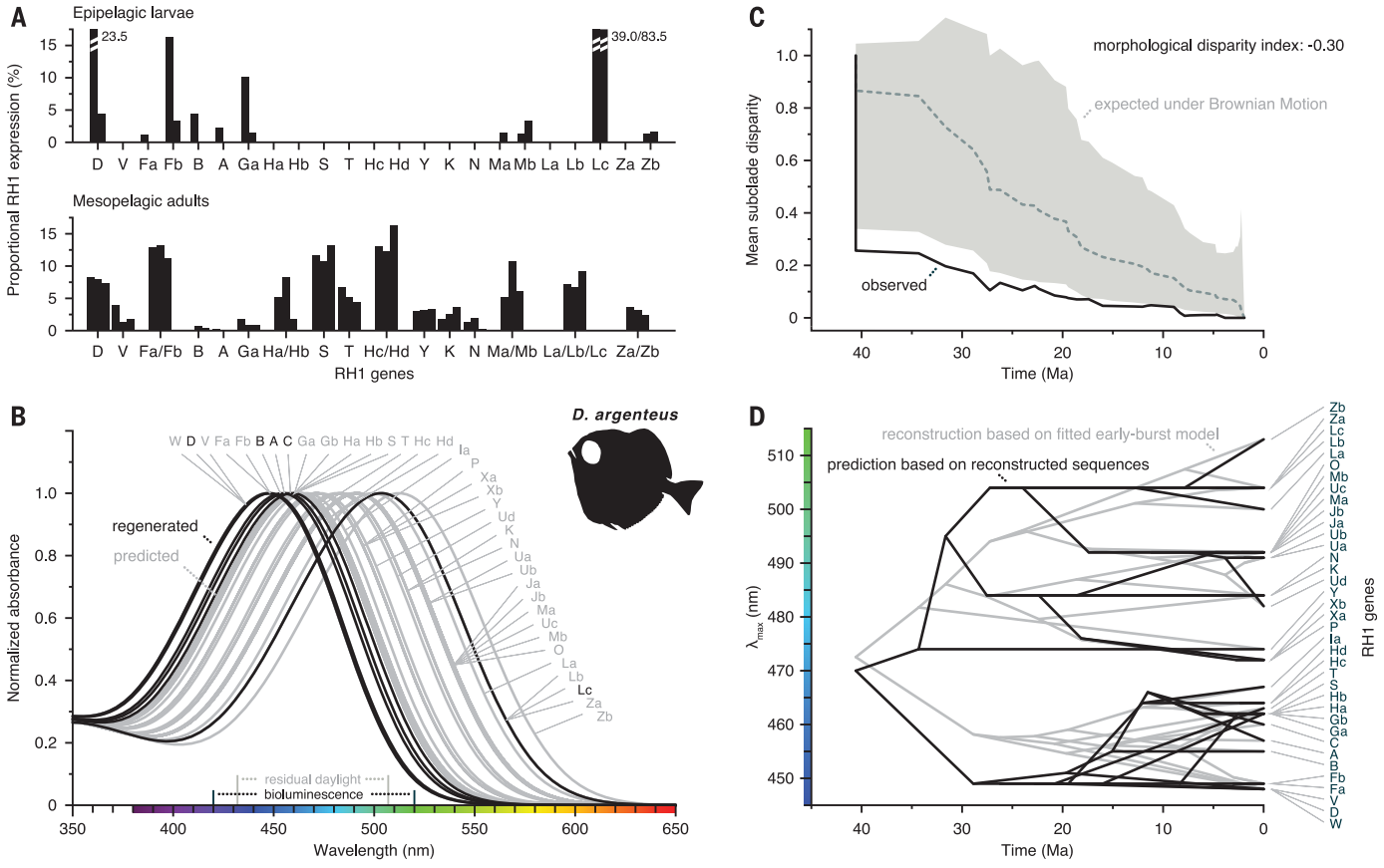

Fig. 2. Molecular function of rod photoreceptors in the silver spinyfin. (**A**) Expression of *RH1* genes in the retina of epipelagic larvae (upper panel) and adults (lower panel). (**B**) Peak spectral sensitivities (λ_{max}) of 37 (out of 38) RH1s of *D. argenteus* on the basis of in vitro protein regenerations (black) and subsequent key tuning-site predictions (gray). (**C**) Reconstruction of mean subclade disparity through time in λ_{max} values for the RH1s of *D. argenteus*, supporting an early-burst (EB) scenario of diversification (Akaike information criterion AIC_{EB} = 236.4) over time-homogeneous diversification [Brownian motion (BM); AIC_{BM} = 244.9] or selection toward an optimal value of λ_{max} [Ornstein-Uhlenbeck model (OU), not shown; AIC_{OU} = 246.9]. Ma, million years. (**D**) Functional divergence through time of λ_{max} values according to predicted λ_{max} values for reconstructed ancestral sequences (black) and ancestral λ_{max} values reconstructed on the basis of an EB model (gray).

spectral tuning of RH1 photopigments via functional shifts in λ_{max} (*1*, *3*). Our ancestral state reconstruction revealed that 25 of these 27 known key spectral tuning sites have been altered across teleosts (Fig. 3 and fig. S4), and at 18 of these sites, the same amino acid substitutions have occurred repeatedly in different lineages (table S5). The lineage-specific *RH1* expansion within Diretmidae alone gave rise to a set of genes differing in 24 key spectral tuning sites (tables S5 and S6). In addition, the *RH1* genes of Diretmidae show by far the highest nonsynonymous to synonymous substitution rate ratios (*dN*/*dS*) across all teleost *RH1*s (Fig. 3B and table S7), suggesting that the extensive occurrence of parallel substitutions was driven by adaptive sequence evolution.

Using *D. argenteus* as an example, we tested whether the deep-sea fish *RH1* expansions translate into differently tuned photopigments. Predictions on the basis of regenerated proteins and molecular dynamics simulations (*8*) revealed that the *D. argenteus* RH1s cover a λ_{max} range of 447 to 513 nm and 444 to 519 nm, respectively (Fig. 2B, figs. S5 to S8, and tables S8 to S10). This peak-to-peak spectral range is much broader than that commonly found for RH1 in other deep-sea fishes (λ_{max} = 477 to 490 nm) and includes the most blueshifted rod opsins known for vertebrates (*14*). However, this spectral range largely overlaps with both the waveband of bioluminescent light emitted by deep-sea organisms (λ = 420 to 520 nm) (*5*) and the residual daylight at a depth of 500 m (λ = 432 to 507 nm) (*15*). A function-through-time analysis inferred that the ancestral Diretmidae RH1 photopigment had a λ_{max} of ~472 nm, similar to the spectral peak of the rod photopigment in most extant deep-sea fishes (*14*). A subsequent gene duplication event led to two versions of *RH1* that diverged rapidly in spectral sensitivity (λ_{max} ~ 457 and 482 nm), which gave rise to all further *RH1*s (Fig. 2, C and D). The emergence of the blueshifted clade was likely caused by the loss of a key disulfide bridge between amino acid positions 111 and 188 (Fig. 3C, table S10, and movies S1 and S2), extending the list of known tuning sites.

The vastly expanded opsin gene repertoire of Diretmidae is therefore noteworthy, especially in the context of its retinal anatomy: The ventral (upward-directed) retina of *D. argenteus* contains extremely long rods as part of a multibank retina (*16*, *17*). Placing just the shortest- or the longest-tuned *D. argenteus* visual pigments within these rods results in very broad absorptance spectra that would not only overlay the spectra of the remaining RH1 pigments but would also maximize photon capture (fig. S9). This is also the case for the other examples of deep-sea fishes that have retinae with multiple rod opsins (e.g., Myctophidae and Stylephoridae); these species also possess very long photoreceptors and, in some cases, multibank retinae (*6*, *7*). Notwithstanding the potential

Downloaded from http://science.sciencemag.org/ on May 9, 2019

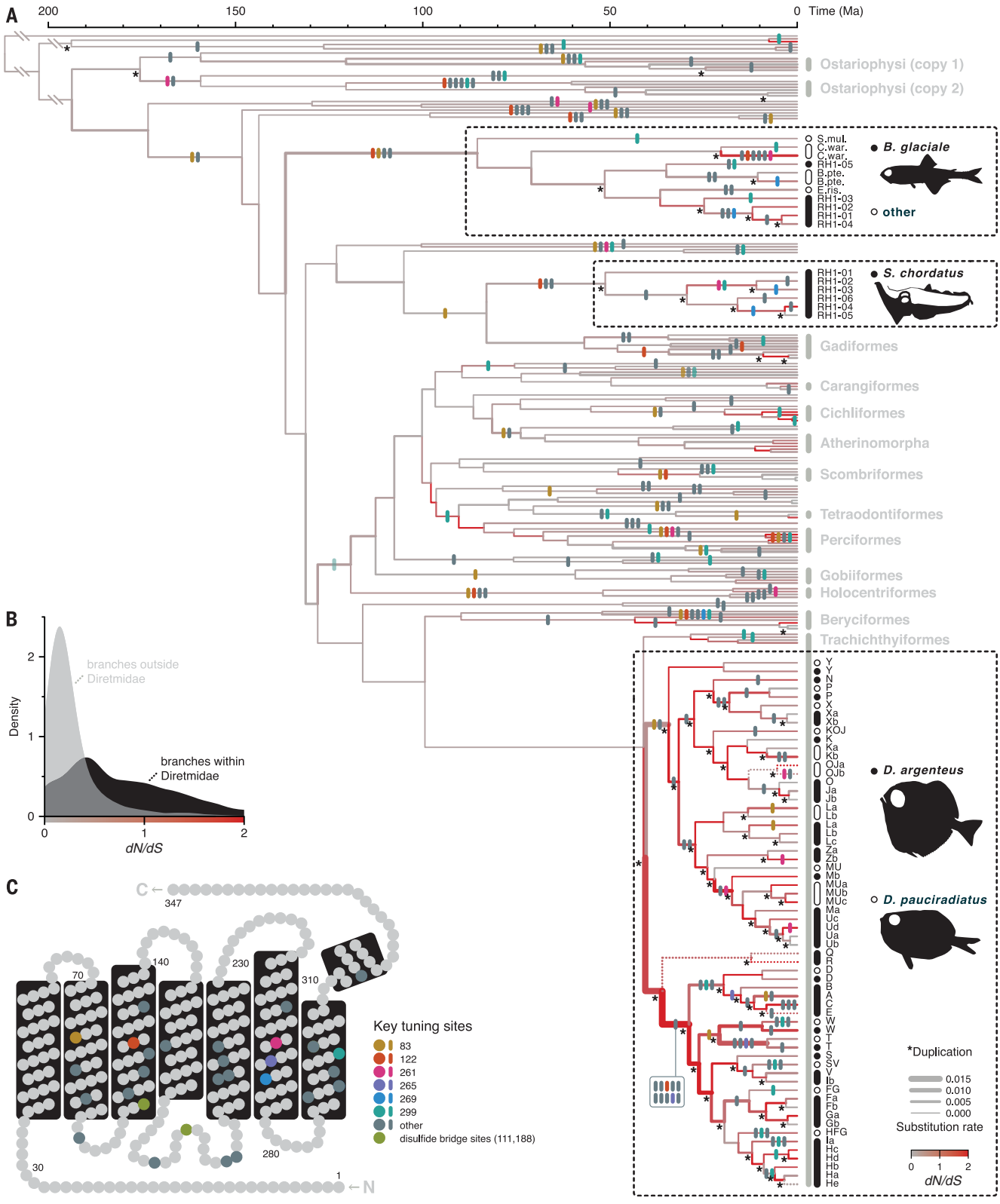

Fig. 3. Evolution and functional diversification of RH1 in deep-sea fishes. (**A**) Time-calibrated gene tree based on teleost *RH1*s, demonstrating lineage-specific duplications in three deep-sea fish lineages. Vertical bars indicate amino acid substitutions in key spectral tuning sites (*1*, *3*). Asterisks denote gene duplication events. The branches in the gene tree are color-coded according to the rate of nonsynonymous to synonymous substitutions (*dN*/*dS*); each branch's thickness corresponds to the reconstructed substitution rate. (**B**) Distribution of the per-branch *dN*/*dS* values within the *RH1*s of Diretmidae compared with that of all other branches in the teleost *RH1* gene tree, based on ancestral sequence reconstructions. (**C**) Basic model of the RH1 protein showing its seven transmembrane helices and the positions of known key spectral tuning sites, including the disulfide bridge reported here.

Downloaded from http://science.sciencemag.org/ on May 9, 2019

for any single photoreceptor to sample all available light, it is worthwhile to explore the possible functions of multiple spectral sensitivities in this environment. Five scenarios, which are not necessarily mutually exclusive, could explain the *RH1* proliferation:

1) The sensitivity of individual photoreceptors may be (further) broadened by coexpression of multiple, differently tuned RH1s across the ambient light spectrum. As a result, absolute sensitivity in scotopic conditions may increase, as proposed for cone coexpression in nocturnal mammals (*18*).

2) Sensitivity may be increased through summing the outputs of photoreceptors that contain different spectral sensitivities, regardless of whether they contain one or more RH1s (*6*).

3) Color discrimination may be possible if different spectral classes or combinations thereof are compared through an opponent process (*16*). Although color discrimination is representative of "normal" color vision, its mediation by rods containing RH1s rather than by cones would be distinctive (*19*, *20*).

4) Each spectral sensitivity or set of sensitivities may be hardwired to a specific behavior—e.g., identification of a particular bioluminescent flash—a process termed wavelength-specific or unconventional color vision in other animals (*21*).

5) The range of spectral sensitivities acts as a store of solutions that can be "pulled off the shelf" at different developmental stages or placed in different retinal regions to optimize the sensitivity and/or contrast of objects (*21*).

Supporting the existence of purely rod-based color vision in deep-sea fishes (scenarios 3 and 4), members of the deep-sea lineages with expanded *RH1* repertoires have rod photoreceptors with different spectral sensitivities and additional yellow spectral filters within the eye. These filters have been suggested to enhance color discrimination or, at minimum, contrast (*22*, *23*). Color vision in the deep sea may be advantageous for recognition of spectrally diverse bioluminescent spectra (*5*). For example, it may help break bioluminescent camouflage against downwelling light to facilitate the identification of conspecifics or prey (*16*).

Although we are currently unable to behaviorally test any of these possibilities, theoretical visual models from the perspective of *D. argenteus* enable us to make some predictions (fig. S10 and table S11). Contrast detection of a black object (e.g., a fish silhouette) or a bioluminescent light source (e.g., a decapod prey) against the residual daylight requires only a single RH1 photopigment. However, for optimal detection of a black object, that pigment must be exactly matched to the background illumination, whereas a bioluminescent object demands a sensitivity slightly longer than the peak emission of the bioluminescence. Hence, several differently tuned photopigments would be beneficial for the detection of different bioluminescence sources (fig. S10B). Conversely, if two bioluminescent signals were to be distinguished from one another (a form of color vision), maximum discrimination would ideally be achieved using two photopigments matched to each bioluminescent emission. None of the models predict why having 14 functional sensitivities is useful; however, they do suggest that an exact sensitivity match to each specified task is an advantage. Possessing an adaptable system (as suggested in scenario 5) during ontogeny or to optimize upward, downward, and side-facing vision may require this sort of spectral class diversity.

An interesting parallel exists among otherwise-monochromatic cephalopods: The abraliopsid squids also express multiple visual pigment types in multibank retinae and use differently colored bioluminescent signals during seasonal mating (*24*). Regardless of whether bioluminescent signaling in the deep has driven the extreme diversity of spectral sensitivities in deep-sea fish, our findings help redefine the current paradigm of vertebrate vision in terms of the role of rod photoreceptors.

REFERENCES AND NOTES

1. S. Yokoyama, *Annu. Rev. Genomics Hum. Genet.* **9**, 259–282 (2008).
2. J. N. Lythgoe, *The Ecology of Vision* (Clarendon Press, 1979).
3. D. M. Hunt, S. P. Collin, in *Evolution of Visual and Non-Visual Pigments*, D. M. Hunt, M. W. Hankins, S. P. Collin, N. J. Marshall, Eds. (Springer Series in Vision Research, Springer, 2014), pp. 163–217.
4. R. H. Douglas, T. W. Cronin, in *The Ecology of Animal Senses*, G. von der Emde, E. Warrant, Eds. (Springer, 2016), pp. 169–203.
5. E. A. Widder, *Science* **328**, 704–708 (2010).
6. E. J. Warrant, N. A. Locket, *Biol. Rev.* **79**, 671–712 (2004).
7. H. J. Wagner, E. Fröhlich, K. Negishi, S. P. Collin, *Prog. Retin. Eye Res.* **17**, 637–685 (1998).
8. Materials and methods are available as supplementary materials.
9. F. Cortesi *et al.*, *Proc. Natl. Acad. Sci. U.S.A.* **112**, 1493–1498 (2015).
10. J. M. Morrow *et al.*, *J. Exp. Biol.* **220**, 294–303 (2017).
11. A. Kelber, M. Vorobyev, D. Osorio, *Biol. Rev.* **78**, 81–118 (2003).
12. R. Futahashi *et al.*, *Proc. Natl. Acad. Sci. U.S.A.* **112**, E1247–E1256 (2015).
13. M. L. Porter *et al.*, *Integr. Comp. Biol.* **53**, 39–49 (2013).
14. R. H. Douglas, J. C. Partridge, N. J. Marshall, *Prog. Retin. Eye Res.* **17**, 597–636 (1998).
15. S. Johnsen, *Annu. Rev. Mar. Sci.* **6**, 369–392 (2014).
16. E. J. Denton, N. A. Locket, *J. Mar. Biol. Assoc. U. K.* **69**, 409–435 (1989).
17. O. Munk, *Videnskab. Meddr. Dansk. Naturh. Foren.* **129**, 73–80 (1966).
18. L. Peichl, *Anat. Rec.* **287A**, 1001–1012 (2005).
19. L. S. Roth, A. Kelber, *Proc. R. Soc. B* **271** (suppl. 6), S485–S487 (2004).
20. C. A. Yovanovich *et al.*, *Philos. Trans. R. Soc. B* **372**, 20160066 (2017).
21. J. Marshall, K. L. Carleton, T. Cronin, *Curr. Opin. Neurobiol.* **34**, 86–94 (2015).
22. F. de Busserolles *et al.*, *Brain Behav. Evol.* **85**, 77–93 (2015).
23. J. C. Partridge, S. N. Archer, J. Vanoostrum, *J. Mar. Biol. Assoc. U. K.* **72**, 113–130 (1992).
24. M. Michinomae, H. Masuda, M. Seidou, Y. Kito, *J. Exp. Biol.* **193**, 1–12 (1994).

ACKNOWLEDGMENTS

We thank A. Bentley, M. Berenbrink, W.-S. Chung, A. Indermaur, X. Irigoien, S. Kaartvedt, L. Kalous, M. D. MacDonald, J. Peterka, G. Phillips, J. Y. Poulsen, E. S. Riiser, A. Rostad, O. Roth, A. G. Salvanes, H. T. Baalsrud, and L. Frey (HBOI/Blue Turtle Engineering) for help in the field and/or for providing samples; the staff of the Lizard Island Research Station for logistical support; the captains and crews of the research vessels *Seward Johnson*, *Walther Herwig III*, *Sonne*, *G. O. Sars*, *Thuwal*, *Maria S. Merian*, and *Trygve Braarud* for the opportunity to participate and collect samples; the Norwegian Sequencing Centre (NSC), University of Oslo, and the McGill University and Génome Québec Innovation Centre for performing whole-genome sequencing; J. Edson (Queensland Brain Institute), C. Beisel (D-BSSE, Basel), and C. Michell (KAUST) and teams for help with transcriptome sequencing; the Center for scientific computing @ University of Basel (sciCORE), the High-Performance Computing Center at Idaho National Laboratory (supported by the Office of Nuclear Energy of the U.S. DOE and the Nuclear Science User Facilities under contract DE-AC07-05ID14517), and the Abel Supercomputing Cluster [Norwegian metacenter for High Performance Computing (NOTUR) and the University of Oslo] operated by the Research Computing Services group at USIT, the University of Oslo IT department (www.hpc.uio.no/) for computational resources; the Waitt Foundation for Discovery for hosting and support; F. Santini for discussions regarding fossil calibrations; and anonymous referees for insightful comments and suggestions that improved the manuscript.
Funding: This work was funded by the Czech Science Foundation (16-09784Y), the Swiss National Science Foundation (SNF, 166550), and the Basler Stiftung für Experimentelle Zoologie to Z.M.; an SNF Postdoctoral Fellowship (165364) and a UQ Development Fellowship to F.C.; a Future Fellowship (FT110100176) of the Australian Research Council (ARC) and a Discovery Project grant (DP140102117) to W.I.L.D.; the ARC to F.C. and J.M.; the Basler Stiftung für Biologische Forschung to Z.M. and S.M.S; the Research Council of Norway (RCN 222378) to K.S.J.; the Center for Modeling Complex Interactions sponsored by the NIGMS (P20 GM104420) and National Science Foundation EPSCoR Track-II (OIA1736253) to J.S.P.; KAUST to F.d.B.; the NIH (R01EY012146) to D.L.S.; the NIH (R01EY024639) to K.L.C.; The Deep Australia Project ARC LP0775179 to J.M.; and the European Research Council (ERC; CoG "CICHLID~X") and the SNF (156405, 176039) to W.S. **Author contributions:** Z.M., F.C., J.M., and W.S. conceived the study. Mi.M., Ma.M., R.H., K.S.J., S.J., and W.S. planned and led the genome sequencing and provided samples. Z.M., F.C., F.d.B., J.M., and W.S. carried out transcriptome sequencing. Z.M. and F.C. carried out the opsin gene analyses. F.C. and S.M.S. performed the PGLS analyses. Mi.M., Ma.M., O.K.T., and S.J., carried out the genome assemblies and annotations. Mi.M. carried out phylogenetic analyses. K.L.C. performed the regulatory region analyses and visual modeling. W.I.L.D. and J.K.M. carried out the in vitro regeneration and spectral prediction analyses. J.S.P. performed the atomistic molecular simulations, and J.S.P., C.J.B., and D.L.S. generated, analyzed, and interpreted the predictive model. Z.M., F.C., and W.S. wrote the initial manuscript draft, and all authors commented on the manuscript and approved the final version. **Competing interests:** The authors declare no competing interests. **Data and materials availability:** New draft genome sequences from this study are available at the European Nucleotide Archive (ENA) (study accession number: PRJEB30779); transcriptomic data that support the findings of this study have been deposited in GenBank (BioProject ID PRJNA421052). Source files, including custom scripts, have been deposited in GitHub (https://github.com/mmatschiner/opsin_evolution); phylogenetic trees and sequence alignments are available at http://evoinformatics.eu/opsin_evolution.htm. All other data analyzed during this study are included as supplementary materials.

SUPPLEMENTARY MATERIALS

science.sciencemag.org/content/364/6440/588/suppl/DC1
Material and Methods
Supplementary Text
Figs. S1 to S10
Tables S1 to S11
References (*25*–*221*)
Movies S1 and S2

23 September 2018; accepted 16 April 2019
10.1126/science.aav4632

Downloaded from http://science.sciencemag.org/ on May 9, 2019